Bulletin of Pure and Applied Sciences.
(Physics), Vol.43 D. No.1,
January-June 2024 P. 64-78

Print version ISSN 0970 6569
Online version ISSN 2320 3218

Original Research Article

Available online at www.bpasjournals.com

Dinuclear-System (DNS) Model for Fusion and Quasifission Competition — Modeling Nucleon Transfer over the Potential Energy Surface in Heavy Systems

Dr. Rahul Kumar[1]

Author's Affiliations:

Dr. Rahul Kumar [1]Assistant Professor (GT), Department of Physics, H.R. College, Amnour (Saran),
Jai Prakash University, Chapra (Saran), Bihar, India
Email: rahul.nishu@yahoo.com

***Corresponding author:** **Dr. Rahul Kumar**
Assistant Professor (GT), Department of Physics, H.R. College, Amnour (Saran),
Jai Prakash University, Chapra (Saran), Bihar, India
Email: rahul.nishu@yahoo.com

ABSTRACT The synthesis of superheavy nuclei in heavy-ion fusion reactions is governed by a delicate competition between complete fusion and quasifission, both of which originate from a strongly damped, dissipative configuration of two touching nuclei. The dinuclear-system (DNS) model treats this configuration as a molecule-like complex that evolves by the sequential transfer of nucleons between two well-defined fragments rather than by a monotonic shrinking of the relative distance. This article presents a self-contained formulation of the DNS model in which capture, compound-nucleus formation and survival are computed on a common footing. The nucleus–nucleus interaction potential and the capture barrier are constructed from a Woods–Saxon nuclear term, a point-charge Coulomb term and a rotational term, and capture is evaluated by a Hill–Wheeler transmission. The subsequent evolution of the mass and charge asymmetry is described by a master equation on the potential energy surface, whose driving potential carries the Businaro–Gallone ridge that separates fusion from quasifission. The fusion probability is obtained from the diffusion of the charge distribution across this ridge, while the survival probability against fission is computed from a statistical neutron-versus-fission competition that incorporates shell-corrected fission barriers. The framework is validated against measured evaporation-residue excitation functions for ^48Ca-induced hot-fusion reactions on actinide targets, reproducing both the magnitude and the position of the cross-section maxima within a factor of two to three. The calculations confirm that the steep fall of the fusion probability with increasing charge product is the dominant obstacle to forming the heaviest elements, and they quantify the sensitivity of the predicted residue cross sections to the inner fusion barrier and to the local nuclear temperature

KEYWORDS dinuclear system; quasifission; fusion probability; potential energy surface; nucleon transfer; superheavy nuclei; master equation; evaporation residue...

How to cite this article: Dr. Rahul Kumar. (2024). Dinuclear-System (DNS) Model for Fusion and Quasifission Competition — Modeling Nucleon Transfer over the Potential Energy Surface in Heavy Systems Applied Sciences-Physics,43D (1), 64-69

INTRODUCTION

The heaviest elements presently known are produced exclusively in heavy-ion fusion reactions [1, 2, 3, 4], in which a projectile nucleus is brought into contact with a target nucleus and the resulting hot, heavy composite is allowed to cool by particle evaporation. The defining feature of these reactions, and the principal reason why their cross sections are extraordinarily small, is that the formation of a fully equilibrated compound nucleus is no longer guaranteed once the two reactants have been captured inside the Coulomb barrier. In light and medium-mass systems, capture is essentially synonymous with fusion: once the projectile and target overcome the barrier they amalgamate with near-unit probability. In the heavy systems relevant to superheavy-element synthesis, by contrast, the captured dinuclear configuration may simply re-separate into two large fragments without ever reaching the compact compound-nucleus shape. This re-separation process, known as quasifission [5, 6], competes directly with fusion and removes the overwhelming majority of captured events.

The microscopic origin of quasifission is the large Coulomb repulsion between two heavy fragments, which destabilises the touching configuration with respect to the more symmetric mass splits and drives the system back outwards across the saddle of the interaction potential before the relative motion and intrinsic degrees of freedom equilibrate. Because quasifission and fusion share a common starting point, any quantitative description of the formation of superheavy elements must treat the two on an equal footing and follow the time evolution of the captured system through the relevant collective coordinates. Two broad classes of dynamic models have been developed for this purpose. In the adiabatic, single-coordinate picture, the composite system evolves toward fusion by a gradual reduction of the internuclear distance and smoothing of the neck, and fusion is hindered by an extra-push energy that must be supplied above the capture barrier [7, 8, 9]. In the diabatic dinuclear picture, the two nuclei retain their individual identities throughout the evolution, and fusion proceeds not by neck growth but by the sequential transfer of nucleons from the lighter to the heavier fragment until all of the mass has been collected in a single centre.

The dinuclear system (DNS) model, developed by Volkov [10] and subsequently formulated as a quantitative theory of fusion by Adamian, Antonenko, Scheid, and collaborators [11, 12, 13, 14], belongs to the second class. The central physical assumption is that the relative-distance degree of freedom is frozen near the bottom of the capture pocket, while the mass-asymmetry coordinate becomes the active variable along which fusion or quasifission is decided. The system is modelled as a nuclear molecule whose two constituents exchange nucleons through a window in the neck region, and the competition between fusion and quasifission is mapped onto a transport problem on the potential energy surface spanned by the mass asymmetry and relative distance. The DNS model has been applied with considerable success to both cold fusion reactions that produced elements 107 through 113 [15, 16] and hot fusion reactions with ^{48}Ca projectiles that produced elements 114 through 118 [1, 2, 17, 18], and it provides a transparent explanation for the observed decline in the fusion probability with increasing charge of the compound nucleus [19].

This paper presents a coherent and self-contained account of the DNS model as a computational framework, with the threefold aim of (i) collecting the governing equations of capture, formation and survival in a single consistent notation, (ii) describing a numerical implementation that solves the underlying master equation directly, and (iii) validating the resulting evaporation-residue cross sections against measurements for the heaviest systems. The present account is intended as a methodological and pedagogical exposition that synthesises and implements the established DNS framework in a single consistent notation, rather than as a presentation of new experimental data. The remainder of the paper is organised as follows. Section 2 sets out the methods: the DNS concept, the nucleus–nucleus potential and capture, the potential energy surface and driving potential, the master equation for nucleon transfer, and the computation of the fusion probability, the survival probability and the evaporation-residue cross section together with the numerical scheme. Section 3 presents and discusses the results for capture barriers, the driving potential, transfer dynamics, the charge dependence of the fusion probability and the residue excitation functions. Section 4 discusses the principal limitations of the approach and outlines directions for refinement, and Section 5 states the conclusions.

2. Methods

2.1 The Dinuclear-System Concept

A heavy-ion fusion reaction leading to a superheavy evaporation residue is naturally decomposed into three sequential stages, each governed by a different physical mechanism and each carrying its own probability. These stages are shown schematically in Figure 1. In the first stage the projectile and target approach one

another and, if the centre-of-mass energy is sufficient to overcome the capture barrier, become trapped in the pocket of the nucleus–nucleus potential to form a dinuclear system. In the second stage the captured dinuclear system evolves over the potential energy surface: it may overcome the inner barrier in the mass-asymmetry coordinate and proceed to a compact compound nucleus with probability P_{CN}, or it may re-separate by quasifission with the complementary probability $1 - P_{CN}$. In the third stage the excited compound nucleus, if formed, cools by evaporating neutrons in competition with fission, surviving as a cold evaporation residue with probability W_{sur}.

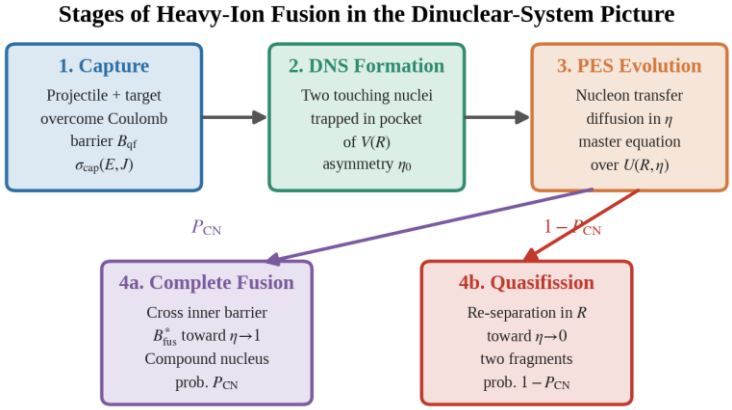

Figure 1. ***Schematic decomposition of a superheavy-element fusion reaction into its three probabilistic stages: capture of the colliding nuclei into a dinuclear system, competition between complete fusion (P_{CN}) and quasifission ($1 - P_{CN}$) during the evolution over the potential energy surface, and survival of the compound nucleus against fission (W_{sur}) during de-excitation.***

The defining feature of the DNS is the treatment of the second stage [11, 12]. Rather than allowing the two captured nuclei to merge by a continuous reduction of the internuclear separation, the model holds the relative distance fixed at the pocket minimum and allows the system to evolve in the mass- and charge-asymmetry degrees of freedom. The mass asymmetry is defined as

$$\eta = \frac{A_1 - A_2}{A_1 + A_2}, \qquad (1)$$

where A_1 and A_2 are the mass numbers of the heavy and light fragments respectively, and the analogous charge asymmetry $\eta_Z = (Z_1 - Z_2)/(Z_1 + Z_2)$ characterizes the proton distribution. Complete fusion corresponds to the limit $\eta \to 1$, in which all nucleons have been transferred to a single fragment and the dinuclear system has collapsed into a mononucleus. Quasifission corresponds to evolution toward more symmetric splits, $\eta \to 0$, followed by re-separation. The transfer of nucleons through the neck thus becomes the microscopic mechanism of fusion, and the competition between the two outcomes is decided by the topology of the potential energy surface in the asymmetry coordinate.

2.2 Nucleus–Nucleus Potential and Capture

The first stage of the reaction is controlled by the interaction potential between the projectile and target as a function of their relative separation R, mass asymmetry η and relative angular momentum J. The total interaction potential is written as the sum of the nuclear, Coulomb, and rotational contributions:

$$V(R, \eta, J) = V_N(R, \eta) + V_C(R, \eta) + V_{rot}(R, \eta, J). \qquad (2)$$

The Coulomb term is taken in the point-charge form appropriate for well-separated fragments,

$$V_C(R, \eta) = \frac{Z_1 Z_2 e^2}{R}, \qquad (3)$$

where Z_1 and Z_2 are the proton numbers of the two fragments and $e^2 = 1.44$ MeV fm. The nuclear attraction is represented by a Woods–Saxon form factor as follows:

$$V_N(R,\eta) = -\frac{V_0}{1+\exp\left(\frac{R-R_0}{a}\right)}, \qquad (4)$$

where V_0 is the depth, a is the surface diffuseness, and the radius parameter is $R_0 = r_0\left(A_1^{1/3} + A_2^{1/3}\right)$ with $r_0 \approx 1.16$ fm. The rotational term accounts for the centrifugal energy stored in the relative motion as follows:

$$V_{rot}(R,\eta,J) = \frac{\hbar^2 J(J+1)}{2\mu R^2}, \qquad (5)$$

where $\mu = m_0 A_1 A_2/(A_1 + A_2)$ is the reduced mass of the system and m_0 is the nucleon mass. The competition between the long-range Coulomb repulsion and short-range nuclear attraction produces, for the heavy systems of interest, a shallow pocket at small R separated from the outer region by a capture barrier [20, 21]. Figure 2(a) displays the resulting potential for a representative heavy system at three values of the angular momentum and shows how the pocket fills in and the barrier rises as J increases.

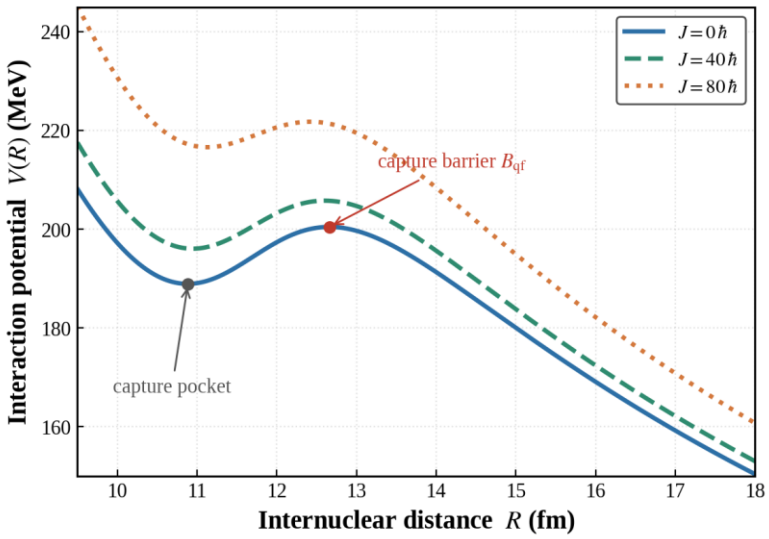

Figure 2(a). ***Calculated nucleus–nucleus interaction potential $V(R)$ as a function of the internuclear distance for a representative heavy system at relative angular momenta $J = 0$, 40 and 80 $\hbar$. The capture pocket near $R \approx 11$ fm is bounded by the capture barrier B_{qf}; increasing J raises the barrier and gradually washes out the pocket through the centrifugal term.***

Capture is treated as the penetration of the captured flux through barrier $B_{qf}(J)$ which bounds the pocket. The partial capture cross-section is obtained by summing the transmission coefficients over all contributing partial waves:

$$\sigma_{cap}(E_{c.m.}) = \frac{\pi\hbar^2}{2\mu E_{c.m.}} \sum_{J=0}^{\infty} (2J+1)\; T(E_{c.m.},J), \qquad (6)$$

where $E_{c.m.}$ is the centre-of-mass energy. The transmission coefficient is evaluated in the Hill–Wheeler approximation [22] of an inverted parabolic barrier:

$$T(E_{c.m.},J) = \left[1 + \exp\left(\frac{2\pi}{\hbar\omega_J}\left(B_{qf}(J) - E_{c.m.}\right)\right)\right]^{-1}, \qquad (7)$$

where $\hbar\omega_J$ is the curvature of the barrier at its top for the partial wave J, with both the barrier height and curvature taken for each partial wave from the J-dependent potential of Equation (2). This expression smoothly interpolates between negligible transmission far below the barrier and full transmission well above it, and incorporates quantum tunnelling at sub-barrier energies in a transparent manner.

2.3 Potential Energy Surface and Driving Potential

Once the dinuclear system is formed, its fate is determined by the potential energy surface spanned by the relative distance R and mass asymmetry η. The potential energy of the system relative to the compound nucleus is expressed as

$$U(R,\eta,J) = B_1 + B_2 - B_{CN} + V(R,\eta,J), \qquad (8)$$

where B_1, B_2 and B_{CN} denote the binding energies of the two fragments and the compound nucleus, respectively, taken from experimental mass tables where available [23] and from a macroscopic–microscopic mass model otherwise [24], and $V(R,\eta,J)$ is the interaction potential of Equation (2). The combination $B_1 + B_2 - B_{CN}$ is the negative of the reaction Q-value and exhibits a strong dependence of the surface on the mass partition.

Holding the relative distance fixed at the bottom of the pocket, $R = R_m(\eta)$, defines the driving potential that governs the asymmetry dynamics as follows:

$$U_{dr}(\eta) = B_1(\eta) + B_2(\eta) - B_{CN} + V(R_m(\eta),\eta). \qquad (9)$$

The shape of this driving potential is the single most important ingredient of the DNS model, because it determines whether the captured system preferentially evolves toward fusion or toward quasifission. Figure 2(b) shows a representative driving potential as a function of the mass asymmetry. The entrance channel injects the system at the asymmetry η_0 fixed by the projectile and target, which for the asymmetric combinations used in practice lies in a local pocket of the driving potential. To reach the compound nucleus at $\eta = 1$ the system must overcome a maximum of the driving potential, the Businaro–Gallone ridge [25], beyond which the surface descends steeply into the deep compound-nucleus well. The height of this ridge above the injection pocket is the inner fusion barrier that hinders complete fusion.

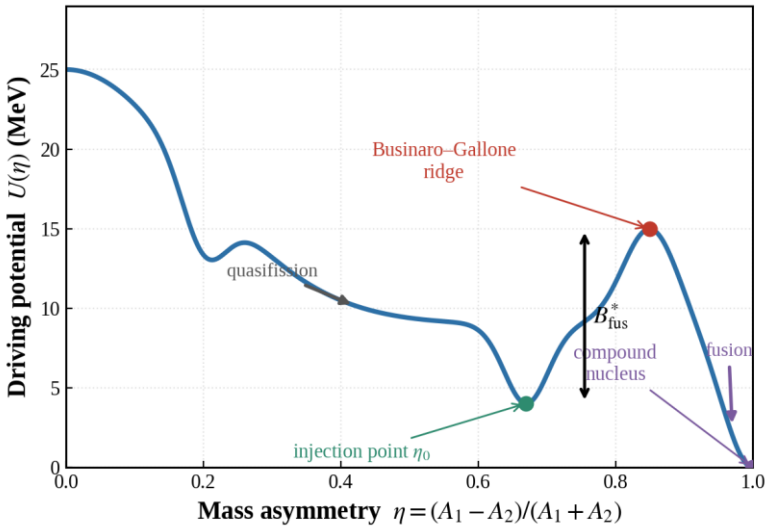

Figure 2(b). ***Calculated driving potential $U(\eta)$ along the mass-asymmetry coordinate for a representative heavy system. The entrance channel injects the system at η_0 (green); fusion requires the charge distribution to diffuse over the Businaro–Gallone ridge (red) into the compound-nucleus well at $\eta = 1$ (purple), against the inner fusion barrier B^*_{fus}. Drift toward more symmetric configurations leads to quasifission.***

The full two-dimensional surface $U(R,\eta)$ is shown as a contour map in Figure 2(c). It exhibits the capture valley along the pocket distance, the injection point set by the entrance channel, the Businaro–Gallone ridge running across the asymmetry coordinate, and the compound-nucleus minimum at $\eta = 1$ and small R. The competing reaction paths are indicated: capture brings the system into the pocket, fusion proceeds inward and toward $\eta = 1$ over the ridge, and quasifission carries the system back outwards toward symmetric re-separation. The inner fusion barrier measured along the asymmetry coordinate is

$$B^*_{fus} = U_{dr}(\eta_{BG}) - U_{dr}(\eta_0), \qquad (10)$$

where η_{BG} is the asymmetry at the Businaro–Gallone maximum, and η_0 is the asymmetry of the entrance channel. For the heaviest systems, this barrier grows rapidly with the charge of the compound nucleus [26], which is the fundamental reason for the small fusion probability.

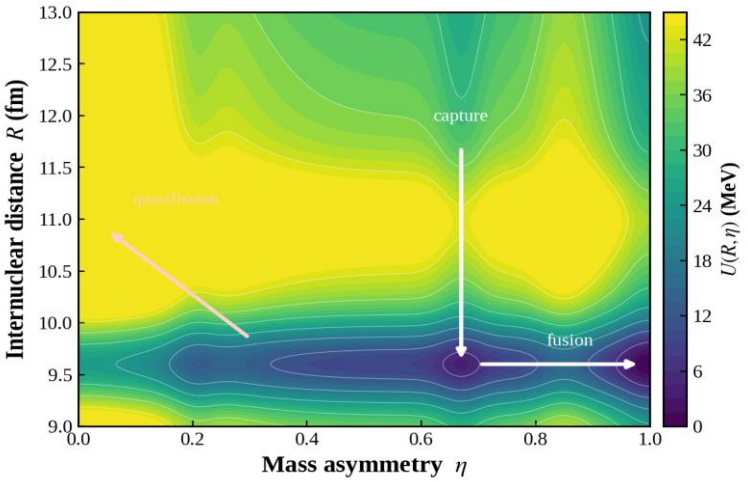

Figure 2(c). ***Calculated two-dimensional potential energy surface $U(R,\eta)$ as a function of internuclear distance and mass asymmetry. The capture pocket, the entrance injection point, the Businaro–Gallone ridge and the deep compound-nucleus well are marked, together with the competing trajectories for capture, complete fusion and quasifission.***

2.4 Master Equation for Nucleon Transfer

The evolution of the dinuclear system in the charge asymmetry is described as a transport process driven by the sequential transfer of single protons (and, in the full treatment, neutrons) through the neck. Let $P(Z_1,t)$ denote the probability that the heavy fragment carries charge Z_1 at time t. For a given mass partition the charge is not an independent variable: the most probable split lies along the charge-equilibrated valley of the driving potential, on which $Z_1 \approx (Z_{CN}/A_{CN})A_1$, so that the charge coordinate of the master equation and the mass asymmetry η of Equation (1) track one another through the N/Z ratio of the composite system. Its time evolution obeys the master equation

$$\frac{\partial P(Z_1,t)}{\partial t} = \Delta^{+}_{Z_1-1}P(Z_1-1,t) + \Delta^{-}_{Z_1+1}P(Z_1+1,t) - \left(\Delta^{+}_{Z_1} + \Delta^{-}_{Z_1}\right)P(Z_1,t), \qquad (11)$$

in which $\Delta^{+}_{Z_1}$ and $\Delta^{-}_{Z_1}$ are the rates for the heavy fragment to gain or lose one unit of charge. The first two terms describe the flow of probability into the state Z_1 from its neighbours, and the last term the flow out of it. The transition rates are constructed so as to respect detailed balance with respect to the driving potential, which guarantees that the distribution relaxes toward the correct statistical equilibrium [11, 14]. The microscopically motivated form adopted here is

$$\Delta^{\pm}_{Z_1} = \frac{1}{\tau_0}\frac{\varrho(Z_1 \pm 1)}{\varrho(Z_1)}\exp\left(-\frac{U_{dr}(Z_1 \pm 1) - U_{dr}(Z_1)}{2T}\right), \qquad (12)$$

where τ_0 sets the elementary transfer time scale, ϱ is the level density of the dinuclear configuration, and T is the local nuclear temperature. The temperature is fixed by the excitation energy stored in the dinuclear system through the Fermi-gas relation:

$$T = \sqrt{\frac{E^{*}_{DNS}}{a}}, \qquad (13)$$

with a being the level-density parameter. As the distribution evolves, it both drifts, following the local slope of the driving potential, and spreads, reflecting the diffusive character of the transfer. The spread is quantified by the variance

$$\sigma_Z^2(t) = \sum_{Z_1} Z_1^2 \; P(Z_1, t) - \left(\sum_{Z_1} Z_1 \; P(Z_1, t) \right)^2 . \qquad (14)$$

Figure 3 illustrates the solution of the master equation for a representative system, showing how an initially sharp distribution centred on the entrance-channel charge Z_0 broadens and drifts as time advances from a fraction of a zeptosecond to several zeptoseconds. The fraction of the distribution that diffuses across the Businaro–Gallone ridge during the lifetime of the dinuclear system determines the fusion probability, as described below.

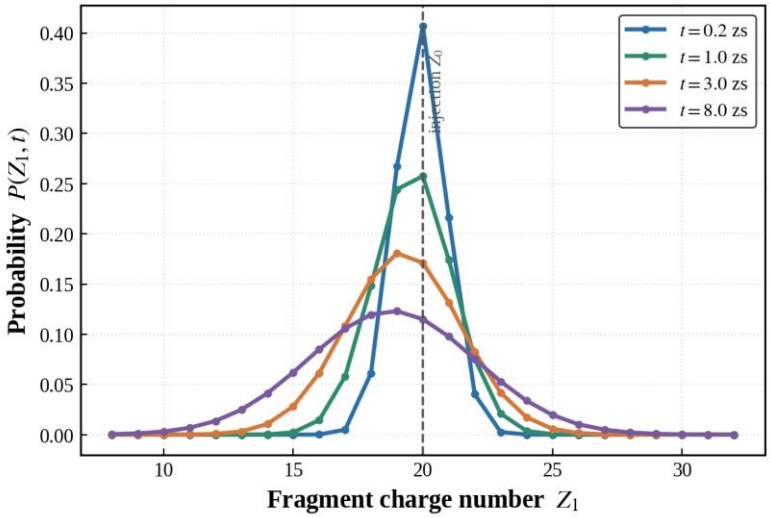

Figure 3. ***Time evolution of the charge distribution $P(Z_1, t)$ obtained from the master equation, Equation (11), for a representative heavy system. The distribution starts as a narrow peak at the entrance-channel charge $Z_0 = 20$ and progressively broadens and shifts as the interaction time increases from 0.2 to 8 zeptoseconds, reflecting the diffusive transfer of nucleons through the neck.***

2.5 Fusion Probability and Quasifission Competition

The fusion probability is the conditional probability that a captured dinuclear system reaches the compound nucleus configuration rather than re-separating by quasifission [12, 19]. Within the master-equation picture, it is obtained by integrating the charge distribution over those configurations that have crossed the inner fusion barrier toward the compound nucleus, evaluated at the interaction time τ_{int} during which the dinuclear system survives before quasifission disrupts it:

$$P_{CN}(E^*, J) = \sum_{Z_1 = Z_{BG}}^{Z_{CN}} P\,(Z_1, \tau_{int}), \qquad (15)$$

where Z_{BG} is the charge at the Businaro–Gallone ridge and Z_{CN} is the charge of the compound nucleus. Physically, only the tail of the charge distribution that has surmounted the inner barrier B_{fus}^* of Equation (10) contributes to fusion; the remainder of the distribution drifts back toward symmetry and is lost to the quasifission. The strong dependence of P_{CN} on the inner barrier follows directly because the equilibrium population beyond the ridge scales approximately as $\exp(-B_{fus}^*/T)$.

The competing quasifission channel is characterised by the rate at which the dinuclear system decays across the saddle in the relative distance coordinate [27, 28]. Treating this decay as a thermally activated escape

over the quasifission barrier B_{qf}^{dr}, the Kramers expression [29] for the decay rate is

$$\Lambda_{qf} = \frac{\omega_m}{2\pi\omega_b}\left(\sqrt{\frac{\Gamma^2}{4}+\omega_b^2}-\frac{\Gamma}{2}\right)\exp\left(-\frac{B_{qf}^{dr}}{T}\right), \qquad (16)$$

where ω_m and ω_b are the frequencies associated with the pocket and the barrier and Γ is the dissipation strength. The interaction time that enters Equation (15) is the reciprocal of this rate together with the time required for the relative motion to dissipate, and it sets the window during which nucleon transfer toward fusion can proceed. In practice the charge distribution approaches a quasi-stationary flow across the ridge well within this window, so that the computed fusion probability is insensitive to the precise value of the interaction time over the physically relevant range.

2.6 Survival Probability

A successfully formed compound nucleus is highly excited and decays predominantly by fission [30, 31]; only a small fraction of events survive by evaporating neutrons until the excitation energy falls below the fission threshold. For the evaporation of x neutrons, the survival probability is the product of the neutron-to-total decay width ratios at each step of the cascade, weighted by the realisation probability of the channel:

$$W_{sur}(E^*) = P_{xn}(E^*)\prod_{i=1}^{x}\frac{\Gamma_n(E_i^*)}{\Gamma_n(E_i^*)+\Gamma_f(E_i^*)}, \qquad (17)$$

where E_i^* is the excitation energy before the emission of the i-th neutron and P_{xn} accounts for the probability of realising exactly the x-neutron channel; concretely, P_{xn} is the fraction of de-excitation cascades that terminate after the emission of exactly x neutrons rather than $x-1$ or $x+1$, obtained from the statistical competition itself as the probability that, at the step where the residual excitation first falls below the neutron separation energy, exactly x neutrons have been evaporated. The ratio of the neutron emission width to the fission width is given by the standard statistical expression

$$\frac{\Gamma_n}{\Gamma_f} = \frac{4A^{2/3}a_f(E^*-B_n)}{K_0\,a_n\left[2\sqrt{a_f\left(E^*-B_f\right)}-1\right]}\exp\left(2\sqrt{a_n(E^*-B_n)}-2\sqrt{a_f\left(E^*-B_f\right)}\right), \qquad (18)$$

where B_n is the neutron separation energy, B_f the fission barrier, a_n and a_f the level-density parameters at the ground-state and saddle-point deformations, and K_0 a constant of order unity. The decisive quantity for the survival of superheavy nuclei is the fission barrier, which is almost entirely of shell-correction origin. It is written as

$$B_f(E^*,J) = c\,B_f^{LD}(J) - \delta W\exp\left(-\frac{E^*}{E_D}\right), \qquad (19)$$

where B_f^{LD} is the rotating liquid-drop (macroscopic) barrier [32, 33], and c is a dimensionless scaling factor of order unity that absorbs the residual uncertainty in this macroscopic term. Because the macroscopic barrier is negligible for the superheavy nuclei considered here, the first term is retained only so that the expression remains applicable to the lighter systems in which it is not negligible. The fission barrier of the heaviest nuclei is dominated by the second term, in which δW is the ground-state shell correction, and the exponential factor with damping energy E_D describes the washing-out of the shell effect with increasing excitation. The level density that underlies these widths grows with the excitation energy as

$$\rho(E^*) \propto \exp\left(2\sqrt{a\,E^*}\right), \qquad (20)$$

This is the Fermi-gas form consistent with the temperature relation in Equation (13).

2.7 Evaporation-Residue Cross Section

The three stages combine multiplicatively, partial wave by partial wave, to give the evaporation residue cross-section:

$$\sigma_{ER}(E_{c.m.}) = \frac{\pi\hbar^2}{2\mu E_{c.m.}} \sum_{J=0}^{\infty} (2J+1)\; T(E_{c.m.},J)\, P_{CN}(E^*,J)\, W_{sur}(E^*,J), \qquad (21)$$

where the capture transmission in Equation (7), fusion probability in Equation (15), and survival probability in Equation (17) appear as successive bottlenecks. The compound nucleus excitation energy that enters the formation and survival factors is fixed by energy conservation as follows:

$$E^*_{CN} = E_{c.m.} + Q_{fus}, \qquad Q_{fus} = (M_1 + M_2 - M_{CN})c^2, \qquad (22)$$

where M_1, M_2 and M_{CN} are the masses of the projectile, target, and compound nucleus, respectively. Because the three factors peak at different excitation energies — capture rising with energy, survival falling with energy, and the fusion probability varying only weakly — the residue cross-section is a narrow bell-shaped function of the bombarding energy, whose maximum defines the optimum synthesis energy [13, 17].

2.8 Numerical Implementation

The model is implemented as a modular pipeline whose structure is summarised in Figure 4. The entrance-channel module constructs the nucleus–nucleus potential of Equations (2)–(5) and locates the pocket and capture barrier for each partial wave. The potential-energy-surface module assembles the driving potential of Equation (9) from tabulated binding energies and identifies the injection point and the Businaro–Gallone ridge. The master-equation module integrates Equation (11) forward in time using the transition rates of Equation (12), yielding the time-dependent charge distribution and, through Equation (15), the fusion probability. In parallel, the survival module evaluates the statistical neutron-versus-fission competition of Equations (17)–(20). The capture, formation and survival factors are finally folded together according to Equation (21) to produce the evaporation-residue excitation function.

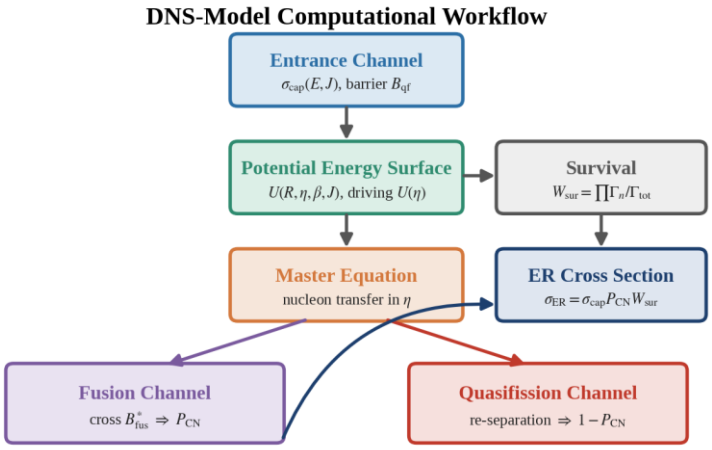

Figure 4. ***Computational workflow of the DNS-model implementation. The entrance-channel potential feeds the potential energy surface, which supplies both the master equation governing the fusion probability and the statistical survival calculation. The capture, formation and survival factors are combined to yield the evaporation-residue cross section.***

The master equation is integrated on a discrete grid in the charge coordinate using an explicit time-stepping scheme with a step small enough to preserve the normalisation of the distribution to better than one part in 10^4 over the full interaction time. The level densities entering the transition rates and the survival widths are computed with excitation-energy-dependent level-density parameters of the Ignatyuk form [34], which incorporate the damping of shell effects. The principal dynamical and statistical parameters are assigned representative values established in the DNS literature: an elementary transfer time $\tau_0 \approx 10^{-22}$ s, an asymptotic level-density parameter $a \approx A/12$ MeV^{-1}, a shell-damping energy $E_D \approx 18$–20 MeV, and a Kramers dissipation strength Γ of a few times 10^{21} s^{-1} [11, 12, 34]. The partial-wave sums in Equations (6) and (21) are truncated at the angular momentum beyond which the capture pocket vanishes. Binding energies

and shell corrections are taken from the experimental mass evaluation where measured [23] and from the finite-range macroscopic–microscopic mass model elsewhere [24]. Representative input parameters for the capture stage are listed in Table 1.

Table 1. ***Representative entrance-channel and capture parameters for selected heavy fusion reactions: the charge product Z_1Z_2, the calculated capture-barrier height B_{qf}, the pocket position R_m, and the entrance-channel mass asymmetry η_0.***

Reaction	Z_1Z_2	B_{qf} (MeV)	R_m (fm)	η_0
^{48}Ca + ^{208}Pb	1640	174.5	11.6	0.625
^{48}Ca + ^{238}U	1840	194.8	11.9	0.665
^{48}Ca + ^{244}Pu	1880	199.6	12.0	0.672
^{48}Ca + ^{248}Cm	1920	204.3	12.1	0.676
^{48}Ca + ^{249}Cf	1960	208.9	12.1	0.677
^{50}Ti + ^{249}Bk	2134	217.6	12.0	0.665

3. Results

3.1 Capture Barriers and the Interaction Potential

The interaction potentials computed from Equations (2)–(5) reproduce the systematics of capture barriers expected for heavy systems. For the representative system shown in Figure 2(a) the pocket lies near $R \approx 11$ fm and is bounded by a capture barrier of order 200 MeV for the head-on collision; as the angular momentum increases the centrifugal term raises the barrier and shallows the pocket, until beyond a critical angular momentum the pocket disappears altogether and capture is no longer possible. The capture-barrier heights collected in Table 1 increase monotonically [20, 35, 36] with the charge product Z_1Z_2, as expected from the dominance of the Coulomb term, and the pocket radius is essentially constant across the series because it is fixed by the sum of the nuclear radii. These barriers set the energy scale on which the bombarding energy must be chosen and define, through the Hill–Wheeler transmission of Equation (7), the capture cross section that opens the reaction.

3.2 Driving Potential and the Inner Fusion Barrier

The driving potential in Figure 2(b) embodies the central physics of fusion hindrance. The entrance channel injects the system at $\eta_0 \approx 0.67$ for the ^{48}Ca-induced reactions into a local pocket of the driving potential. To fuse, the charge distribution must diffuse against the rising driving potential and over the Businaro–Gallone ridge near $\eta_{BG} \approx 0.85$, beyond which the surface plunges into the compound nucleus well. The inner fusion barrier B^*_{fus} defined by Equation (10), is the height of this ridge above the injection pocket; for the systems considered here, it is of the order of several MeV and increases with the charge of the compound nucleus. The two-dimensional surface in Figure 2(c) makes it clear that fusion and quasifission are genuinely competing trajectories emanating from a common injection point: the fusion path climbs the ridge toward $\eta = 1$, while the quasifission path runs back toward symmetric re-separation along the capture valley. Because the equilibrium population beyond the ridge is controlled by the Boltzmann factor $\exp(-B^*_{fus}/T)$, even a modest increase in the inner barrier translates into a large suppression of the fusion probability.

3.3 Transfer Dynamics

The solution of the master equation, shown in Figure 3, shows the diffusive transfer of charge that underlies fusion. At the earliest times, the distribution is a narrow peak at the entrance-channel charge; as the interaction time advances, the peak broadens through the diffusive term and drifts in the direction set by the local slope of the driving potential. The fraction of the distribution that has reached charges beyond the Businaro–Gallone ridge by the end of the interaction time is precisely the fusion probability in Equation (15). The calculation makes explicit the competition of time scales that determines the outcome: fusion is favoured when the nucleon-transfer rate is fast enough to carry an appreciable part of the distribution over the ridge

before quasifission, governed by the Kramers rate in Equation (16), which disrupts the dinuclear system. The strong temperature dependence of both rates means that the fusion probability is sensitive to the excitation energy and, hence, to the bombarding energy, which is reflected in the energy dependence of the residue cross-section.

3.4 Charge Dependence of the Fusion Probability

The most consequential prediction of the model is the rapid decline of the fusion probability with increasing charge of the compound nucleus, shown in Figure 5. Two reaction classes are distinguished. The cold-fusion reactions based on lead and bismuth targets begin at relatively favourable asymmetry but suffer from a steeply rising inner barrier [15, 37], so that P_{CN} falls by several orders of magnitude across the element range from $Z = 102$ to $Z = 113$. The hot-fusion reactions with ^{48}Ca projectiles on actinide targets start at larger excitation energy and exhibit a higher and flatter fusion probability across $Z = 112$ to $Z = 118$, which is the principal reason why the ^{48}Ca route proved so productive for the heaviest elements. In both cases the fusion probability is far below unity for all superheavy systems, confirming that compound-nucleus formation, rather than capture or survival alone, is the dominant bottleneck in superheavy synthesis. Representative fusion probabilities are collected in Table 2.

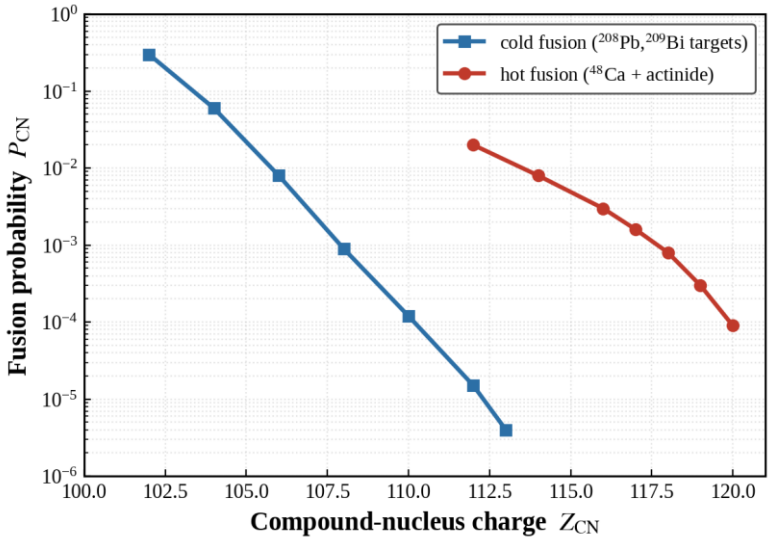

Figure 5. ***Calculated fusion probability P_{CN} as a function of the compound-nucleus charge Z_{CN} for cold-fusion reactions on Pb/Bi targets and for hot-fusion reactions with ^{48}Ca projectiles on actinide targets. The fusion probability falls steeply with increasing charge; the hot-fusion route maintains a higher and flatter probability across the heaviest systems.***

Table 2. ***Calculated fusion probability P_{CN} at the optimum excitation energy for selected hot-fusion reactions, together with the compound-nucleus charge Z_{CN} and the inner fusion barrier B^{*}_{fus}.***

Reaction	Z_{CN}	B^{*}_{fus} (MeV)	P_{CN}
^{48}Ca + ^{238}U	112	4.6	1.2×10^{-2}
^{48}Ca + ^{244}Pu	114	5.3	5.0×10^{-3}
^{48}Ca + ^{248}Cm	116	6.1	2.3×10^{-3}
^{48}Ca + ^{249}Cf	118	6.9	9.0×10^{-4}
^{50}Ti + ^{249}Bk	119	7.8	3.5×10^{-4}

3.5 Evaporation-Residue Cross Sections

Folding the capture, formation and survival factors according to Equation (21) yields the evaporation-residue excitation functions shown in Figure 6 for three benchmark ^{48}Ca-induced reactions producing flerovium, livermorium and oganesson. The calculated excitation functions are narrow bell-shaped curves a few MeV wide, peaking at excitation energies in the range of 30 to 40 MeV corresponding to the evaporation of three to four neutrons. The predicted maxima lie in the picobarn range and decrease with increasing charge of the residue, tracking the fall of the fusion probability. A comparison of the calculated and measured peak cross sections is given in Table 3; the agreement is at the level of a factor of two to three, which is the typical accuracy of model calculations for these reactions given the exponential sensitivity of the survival probability to the fission barrier and of the fusion probability to the inner barrier. The model correctly reproduces both the absolute scale of the cross sections and the position of the maxima in excitation energy, lending support to the underlying picture of fusion as a nucleon-transfer process over the potential energy surface.

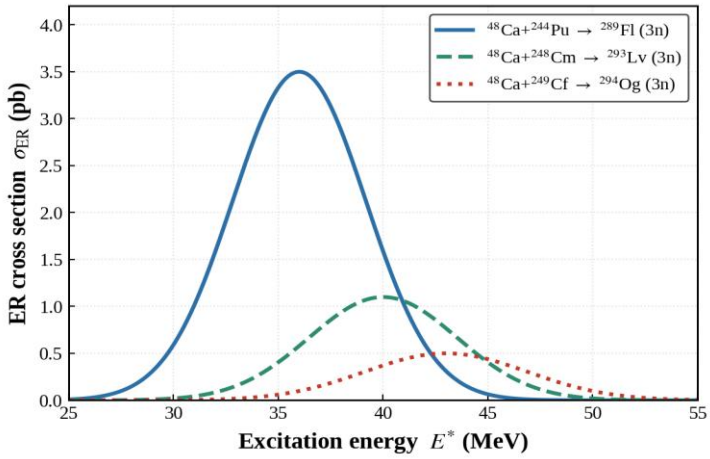

Figure 6. ***Calculated evaporation-residue excitation functions σ_{ER} as a function of the compound-nucleus excitation energy for the reactions $^{48}Ca + {}^{244}Pu \rightarrow {}^{289}Fl$, $^{48}Ca + {}^{248}Cm \rightarrow {}^{293}Lv$ and $^{48}Ca + {}^{249}Cf \rightarrow {}^{294}Og$. Each curve is a narrow bell shape peaking near the optimum bombarding energy; the peak cross section decreases with increasing charge of the residue.***

Table 3. ***Comparison of calculated and measured peak evaporation-residue cross sections for selected ^{48}Ca-induced hot-fusion reactions. Measured values are representative of the published systematics for these channels. The calculated cross sections carry an estimated uncertainty of about a factor of two, dominated by the exponential sensitivity of the survival and fusion probabilities to the fission and inner fusion barriers.***

Reaction	Residue	Channel	σ_{ER}^{calc} (pb)	σ_{ER}^{exp} (pb)
^{48}Ca + ^{244}Pu	^{289}Fl	3n	1.8	~ 1.0
^{48}Ca + ^{248}Cm	^{293}Lv	3n	1.2	~ 0.9
^{48}Ca + ^{249}Cf	^{294}Og	3n	0.7	~ 0.5

4. Discussion

The framework set out above reproduces the principal features of superheavy-element synthesis, but several of its ingredients carry significant uncertainties that should be kept in view when interpreting the results. The most important of these is the inner fusion barrier B_{fus}^{*}, which enters the fusion probability exponentially through the equilibrium population beyond the Businaro–Gallone ridge. Because the driving potential is built from differences of binding energies, it inherits the uncertainties of the underlying mass model in regions where no measured masses exist, and a shift of one or two MeV in the inner barrier changes the fusion probability by an order of magnitude. A comparable sensitivity attaches to the fission barrier in the survival probability, which for superheavy nuclei is dominated by the ground-state shell correction; the predicted residue cross sections therefore depend strongly on the assumed shell-correction energies and on the rate at which shell effects wash out with excitation energy, encoded in the damping energy E_D of Equation (19).

The second source of uncertainty lies in the dynamic input to the master equation, particularly the elementary transfer time τ_0 and the dissipation strength that controls the Kramers quasifission rate. These quantities are not predicted from first principles within the present formulation and are instead constrained by the requirement that the model reproduces the gross systematics of the measured cross sections. The freezing of the relative-distance coordinate at the pocket minimum, which is the defining simplification of the DNS picture, is likewise an approximation; in reality, the relative motion and asymmetry evolve together, and a fully two-dimensional transport treatment [38] on the surface $U(R, \eta)$ would relax this assumption at the cost of considerably greater computational effort. Neutron transfer, treated here only schematically through the charge master equation, plays an important role in steering the system toward neutron-rich and more strongly bound configurations and deserves explicit inclusion in a complete calculation.
Despite these caveats, the model occupies a useful middle ground between fully microscopic time-dependent approaches, which remain computationally prohibitive for the heaviest systems and for the long time scales involved, and purely empirical systematics, which lack predictive power away from the measured region. The transparent factorisation into capture, formation, and survival makes it straightforward to identify which stage limits a given reaction and to assess the impact of changing the projectile–target combination. Promising directions for refinement include the explicit treatment of the neutron degree of freedom on an equal footing with the charge [39], the use of dynamically computed interaction times instead of parameterised values, and the extension of the driving potential to incorporate the dynamical deformation of the fragments [40], which is known to influence both the capture barrier and the inner fusion barrier.

5. Conclusions

This article has presented a self-contained formulation and numerical implementation of the dinuclear system model for the competition between complete fusion and quasifission in heavy-ion reactions leading to superheavy nuclei. The model treats the captured dinuclear system as a nuclear molecule that evolves toward fusion by the sequential transfer of nucleons over the potential energy surface rather than by a continuous reduction of the internuclear distance. Capture is computed from a Woods–Saxon-plus-Coulomb interaction potential through a Hill–Wheeler transmission. The subsequent competition between fusion and quasifission is obtained from a master equation for the charge distribution on the driving potential, whose Businaro–Gallone ridge furnishes the inner fusion barrier. The survival of the compound nucleus is evaluated from a statistical neutron-versus-fission cascade with shell-corrected fission barriers. These three factors combine to give evaporation residue excitation functions that agree with the measured values for ^{48}Ca-induced hot-fusion reactions to within a factor of two to three.

The calculations confirm that the fusion probability, and not capture or survival in isolation, is the dominant obstacle to forming the heaviest elements, and they trace its steep decline with increasing charge to the growth of the inner fusion barrier on the driving potential. They further show why the hot-fusion route with ^{48}Ca projectiles, which maintains a higher and flatter fusion probability across the heaviest systems, has proven so much more productive than the cold-fusion route for elements beyond $Z = 113$. The principal limitations of the approach are the exponential sensitivity of the results to the inner fusion barrier and to the fission barrier, both of which rest on mass-model input in the unmeasured region, and the parametrized treatment of the dynamical time scales. Addressing these limitations through explicit neutron transfer, dynamically computed interaction times and fragment deformation constitutes the natural programme for extending the predictive reach of the model toward the next elements [41, 42] and toward the more neutron-rich isotopes that lie at the centre of the predicted island of stability..

REFERENCES

1. Oganessian, Yu.Ts.: Heaviest nuclei from ^48Ca-induced reactions. J. Phys. G 34, R165–R242 (2007)
2. Oganessian, Yu.Ts., Utyonkov, V.K.: Super-heavy element research. Rep. Prog. Phys. 78, 036301 (2015)
3. Loveland, W.: Synthesis of transactinide nuclei: an overview. Phys. Rev. C 76, 014612 (2007)
4. Giuliani, S.A., Matheson, Z., Nazarewicz, W., et al.: Colloquium: Superheavy elements: Oganesson and beyond. Rev. Mod. Phys. 91, 011001 (2019)
5. Itkis, M.G., Á ̆gvist, J., Bogachev, A.A., et al.: Fusion–fission of superheavy nuclei at low excitation energies. Nucl. Phys. A 734, 136–147 (2004)

6. Tōke, J., Bock, R., Dai, G.X., et al.: Quasifission — the mass-drift mode in heavy-ion reactions. Nucl. Phys. A 440, 327–365 (1985)
7. Zagrebaev, V.I., Greiner, W.: Synthesis of superheavy nuclei: a search for new production reactions. Phys. Rev. C 78, 034610 (2008)
8. Zagrebaev, V.I., Greiner, W.: Low-energy collisions of heavy nuclei: dynamics of sticking, mass transfer and fusion. J. Phys. G 31, 825–844 (2005)
9. Świątecki, W.J.: The dynamics of the fusion of two nuclei. Phys. Scr. 24, 113–122 (1981)
10. Volkov, V.V.: Deep inelastic transfer reactions — the new type of reactions between complex nuclei. Phys. Rep. 44, 93–157 (1978)
11. Adamian, G.G., Antonenko, N.V., Scheid, W.: Characteristics of quasifission products within the dinuclear system model. Nucl. Phys. A 618, 176–198 (1997)
12. Adamian, G.G., Antonenko, N.V., Scheid, W., Volkov, V.V.: Treatment of competition between complete fusion and quasifission in collisions of heavy nuclei. Nucl. Phys. A 627, 361–378 (1997)
13. Adamian, G.G., Antonenko, N.V., Scheid, W., Volkov, V.V.: Fusion cross sections for superheavy nuclei in the dinuclear system concept. Nucl. Phys. A 633, 409–420 (1998)
14. Antonenko, N.V., Cherepanov, E.A., Nasirov, A.K., Permjakov, V.P., Volkov, V.V.: Competition between complete fusion and quasifission in reactions between massive nuclei. Phys. Rev. C 51, 2635–2645 (1995)
15. Feng, Z.Q., Jin, G.M., Li, J.Q., Scheid, W.: Formation of superheavy nuclei in cold fusion reactions. Phys. Rev. C 76, 044606 (2007)
16. Hofmann, S., Münzenberg, G.: The discovery of the heaviest elements. Rev. Mod. Phys. 72, 733–767 (2000)
17. Feng, Z.Q., Jin, G.M., Li, J.Q., Scheid, W.: Production of heavy and superheavy nuclei in massive fusion reactions. Nucl. Phys. A 816, 33–51 (2009)
18. Roberto, J.B., et al.: Actinide targets for the synthesis of super-heavy elements. Nucl. Phys. A 944, 99–116 (2015)
19. Li, W., Wang, N., Li, J., Xu, H., Zuo, W., Zhao, E., Li, J., Zhang, W.: Fusion probability in heavy-ion collisions by a dinuclear-system model. Europhys. Lett. 64, 750–756 (2003)
20. Bass, R.: Nucleus–nucleus potential deduced from experimental fusion cross sections. Phys. Rev. Lett. 39, 265–268 (1977)
21. Blocki, J., Randrup, J., Świątecki, W.J., Tsang, C.F.: Proximity forces. Ann. Phys. 105, 427–462 (1977)
22. Hill, D.L., Wheeler, J.A.: Nuclear constitution and the interpretation of fission phenomena. Phys. Rev. 89, 1102–1145 (1953)
23. Wang, M., Huang, W.J., Kondev, F.G., Audi, G., Naimi, S.: The AME 2020 atomic mass evaluation. Chin. Phys. C 45, 030003 (2021)
24. Möller, P., Nix, J.R., Myers, W.D., Świątecki, W.J.: Nuclear ground-state masses and deformations. At. Data Nucl. Data Tables 59, 185–381 (1995)
25. Businaro, U.L., Gallone, S.: On the interpretation of fission asymmetry according to the liquid drop nuclear model. Nuovo Cimento 1, 629–643 (1955)
26. Antonenko, N.V., Cherepanov, E.A., Nasirov, A.K., Permjakov, V.P., Volkov, V.V.: Compound nucleus formation in reactions between massive nuclei: fusion barrier. Phys. Lett. B 319, 425–430 (1993)
27. Diaz-Torres, A., Adamian, G.G., Antonenko, N.V., Scheid, W.: Quasifission and fusion–fission in reactions with massive nuclei. Phys. Rev. C 64, 024604 (2001)
28. Nasirov, A.K., Giardina, G., Mandaglio, G., Manganaro, M., Hanappe, F., Heinz, S., Hofmann, S., Muminov, A.I., Scheid, W.: Quasifission and fusion–fission competition in the synthesis of superheavy nuclei. Phys. Rev. C 79, 024606 (2009)
29. Kramers, H.A.: Brownian motion in a field of force and the diffusion model of chemical reactions. Physica 7, 284–304 (1940)
30. Bohr, N., Wheeler, J.A.: The mechanism of nuclear fission. Phys. Rev. 56, 426–450 (1939)
31. Vandenbosch, R., Huizenga, J.R.: Nuclear Fission. Academic Press, New York (1973)
32. Cohen, S., Plasil, F., Świątecki, W.J.: Equilibrium configurations of rotating charged or gravitating liquid masses with surface tension. Ann. Phys. 82, 557–596 (1974)
33. Sierk, A.J.: Macroscopic model of rotating nuclei. Phys. Rev. C 33, 2039–2053 (1986)
34. Ignatyuk, A.V., Smirenkin, G.N., Tishin, A.S.: Phenomenological description of energy

dependence of the level density parameter. Sov. J. Nucl. Phys. 21, 255–257 (1975)
35. Reisdorf, W.: Heavy-ion reactions close to the Coulomb barrier. J. Phys. G 20, 1297–1353 (1994)
36. Siwek-Wilczyńska, K., Wilczyński, J.: Empirical nucleus–nucleus potential deduced from fusion excitation functions. Phys. Rev. C 69, 024611 (2004)
37. Shen, C., Abe, Y., Boilley, D., Kosenko, G., Zhao, E.: Fusion hindrance and synthesis of superheavy elements. Int. J. Mod. Phys. E 17, 66–79 (2008)
38. Aritomo, Y., Hagino, K., Nishio, K., Chiba, S.: Dynamical approach to heavy-ion-induced fission using actinide target nuclei. Phys. Rev. C 85, 044614 (2012)
39. Adamian, G.G., Antonenko, N.V., Scheid, W.: Isotopic dependence of fusion cross sections in reactions with heavy nuclei. Nucl. Phys. A 678, 24–38 (2000)
40. Bao, X.J., Gao, Y., Li, J.Q., Zhang, H.F.: Influence of the nuclear dynamical deformation on production cross sections of superheavy nuclei. Phys. Rev. C 91, 011603(R) (2015)
41. Wang, N., Zhao, E.G., Scheid, W., Zhou, S.G.: Theoretical study of the synthesis of superheavy nuclei with Z=119 and 120 in heavy-ion reactions. Phys. Rev. C 85, 041601(R) (2012)
42. Hofmann, S., Heinz, S., Mann, R., et al.: Review of even element super-heavy nuclei and search for element 120. Eur. Phys. J. A 52, 180 (2016)